Inorg. Chem. **2007**, *46*, 9988–9997

Inorganic Chemistry
Article

Mono- versus Bis-chelate Formation in Triazenide and Amidinate Complexes of Magnesium and Zinc

Nonsee Nimitsiriwat,[†] Vernon C. Gibson,[*,†] Edward L. Marshall,[*,†] Pittaya Takolpuckdee,[†] Atanas K. Tomov,[†] Andrew J. P. White,[†] David J. Williams,[†] Mark R. J. Elsegood,[‡] and Sophie H. Dale[‡]

Department of Chemistry, Imperial College London, South Kensington Campus, London SW7 2AZ, U.K., and Chemistry Department, Loughborough University, Loughborough LE11 3TU, U.K.

Received May 31, 2007

Magnesium and zinc complexes of the monoanionic ligands *N*,*N*′-bis(2,6-di-isopropylphenyl)triazenide, L^1, *N*,*N*′-bis(2,6-di-isopropylphenyl)acetamidinate, L^2, and *N*,*N*′-bis(2,6-di-isopropylphenyl)*tert*-butylamidinate, L^3, have been synthesized, but only L^3 possesses sufficient steric bulk to prevent bis-chelation. Hence, the reaction of L^{1}H with excess ZnEt$_2$ leads to the isolation of (L^1)$_2$Zn, **1**; L^{1}H also reacts with Bu$_2$Mg in Et$_2$O to afford (L^1)$_2$Mg(Et$_2$O), **2**. Similar reactivity is observed for L^{2}H, leading to the formation of (L^2)$_2$Zn, **3**, and (L^2)$_2$Mg, **4**. The reaction of L^{2}H with ZnR$_2$ may also afford the tetranuclear aggregates $\{$(L^2)Zn$_2$R$_2\}_2$O, **5** (R = Me) and **6** (R = Et). By contrast, the *tert*-butylamidinate ligand was found to exclusively promote mono-chelation, allowing (L^3)ZnCl(THF), **7**, [(L^3)Zn(μ-Cl)]$_2$, **8**, (L^3)ZnN(SiMe$_3$)$_2$, **9**, (L^3)Mg^{i}Pr(Et$_2$O), **10**, and (L^3)Mg^{i}Pr(THF), **11**, to be isolated. X-ray crystallographic analyses of **1**, **2**, **3**, **4**, **5**, **6**, **8**, and **10** indicate that the capacity of L^3 to resist bis-chelation is due to greater occupation of the metal coordination sphere by the *N*-aryl substituents.

Introduction

A key component of homogeneous polymerization catalysts of the general formula LMX is an ancillary ligand (L), which possesses sufficient steric bulk to withstand bis-chelation, as the formation of L$_2$M may represent a deactivation pathway.[1,2] Ideally, however, L should be small enough so as to not overly obstruct the approach of the monomer to the active metal site. The identification of appropriate ligand−metal combinations, which successfully balance ligand size with metal accessibility, should therefore lead to new generations of highly active, yet well-behaved, living polymerization initiators. One example of much contemporary interest is the stabilization of divalent metal centers for the ring-opening polymerization of cyclic esters (zinc,[3−16] magnesium,[4,6−11,17−20] calcium,[21−23] tin,[24−27] and iron[28]), the living polymerization of methacrylates (magnesium[29]) and the copolymerization of epoxides with CO$_2$ (zinc,[30−47] magnesium[48]). Accordingly, monoanionic ligand families

---

[*] To whom correspondence should be addressed. E-mail: v.gibson@imperial.ac.uk (V.C.G.), e.marshall@imperial.ac.uk (E.L.M.).

[†] Imperial College London.

[‡] Loughborough University.

(1) Coates, G. W. *Dalton Trans.* **2002**, 467−475.

(2) Marshall, E. L.; Gibson, V. C. In *Comprehensive Coordination Chemistry II*; McCleverty, J. A., Meyer, T. J., Eds.; Elsevier: London 2004; Vol. 9, pp 1−74.

(3) Cheng, M.; Attygalle, A. B.; Lobkovsky, E. B.; Coates, G. W. *J. Am. Chem. Soc.* **1999**, *121*, 11583−11584.

(4) Chamberlain, B. M.; Cheng, M.; Moore, D. R.; Ovitt, T. M.; Lobkovsky, E. B.; Coates, G. W. *J. Am. Chem. Soc.* **2001**, *123*, 3229−3238.

(5) Rieth, L. R.; Moore, D. R.; Lobkovsky, E. B.; Coates, G. W. *J. Am. Chem. Soc.* **2002**, *124*, 15239−15248.

(6) Chisholm, M. H.; Eilerts, N. W.; Huffman, J. C.; Iyer, S. S.; Pacold, M.; Phomphrai, K. *J. Am. Chem. Soc.* **2000**, *122*, 11845−11854.

(7) Chisholm, M. H.; Huffman, J. C.; Phomphrai, K. *J. Chem. Soc., Dalton Trans.* **2001**, 222−224.

(8) Chisholm, M. H.; Gallucci, J.; Phomphrai, K. *Inorg. Chem.* **2002**, *41*, 2785−2794.

(9) Chisholm, M. H.; Phomphrai, K. *Inorg. Chim. Acta* **2003**, *350*, 121−125.

(10) Chisholm, M. H.; Gallucci, J.; Phomphrai, K. *Inorg. Chem.* **2005**, *44*, 8004−8010.

(11) Dove, A. P.; Gibson, V. C.; Marshall, E. L.; White, A. J. P.; Williams, D. J. *Dalton Trans.* **2004**, 570−578.

(12) Williams, C. K.; Brooks, N. R.; Hillmyer, M. A.; Tolman, W. B. *Chem. Commun.* **2002**, 2132−2133.

(13) Williams, C. K.; Breyfogle, L. E.; Choi, S. K.; Nam, W.; Young, V. G.; Hillmyer, M. A.; Tolman, W. B. *J. Am. Chem. Soc.* **2003**, *125*, 11350−11359.

(14) Jensen, T. R.; Schaler, C. P.; Hillmyer, M. A.; Tolman, W. B. *J. Organomet. Chem.* **2005**, *690*, 5881−5891.

(15) Hill, M. S.; Hitchcock, P. B. *Dalton Trans.* **2002**, 4694−4702.

(16) Birch, S. J.; Boss, S. R.; Cole, S. C.; Coles, M. P.; Haigh, R.; Hitchcock, P. B.; Wheatley, A. E. H. *Dalton Trans.* **2004**, 3568−3574.

(17) Wu, J. C.; Huang, B. H.; Hsueh, M. L.; Lai, S. L.; Lin, C. C. *Polymer* **2005**, *46*, 9784−9792.

10.1021/ic701061q CCC: $37.00

Scheme 1. Selected Monoanionic Ligand Families (from Left to Right: β-Diketiminates, Salicylaldiminates, Aminotroponiminates, Amidinates, and Triazenides)

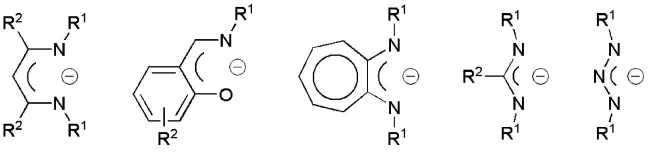

such as β-diketiminates,[49] salicylaldiminates,[50] and aminotroponiminates[51] (Scheme 1) have all been employed in recent times to good effect.

Amidinate ligands have also acquired renewed appeal, mainly as a result of the development of simple synthetic routes to sterically bulky variants.[52−64] Of particular relevance to the study described below, Jordan et al. have shown that the presence of a sizable substituent on the central carbon atom forces the two nitrogen substituents to project further forward, thus improving steric protection of the metal.[65] By contrast, the triazenide family,[66] [RNNNR]$^-$, has received far less recent attention. As noted by Gantzel and Walsh,[67] triazenide ligands are expected to donate less electron density to metal centers than amidinates, an important consideration in the design of Lewis acidic catalysts for coordinative-insertion polymerizations.

Scheme 2. Ligands Employed in This Study

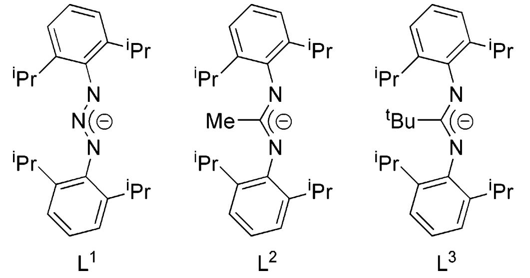

Here, we describe the synthesis and characterization of a series of magnesium and zinc complexes of 2,6-di-isopropylanilido-based triazenide (L^1, Scheme 2) and amidinate (L^2 and L^3) ligands. Our results demonstrate how finely balanced the factors influencing mono- versus bis-chelation can be and should aid the future rational development of single-site, mono-chelated catalysts.

Results and Discussion

Syntheses of Triazenide Complexes. The synthesis of *N*,*N*′-bis(2,6-di-isopropylphenyl)triazene, L^{1}H, was accomplished as shown in Scheme 3.[68,69] Stirring isoamylnitrite with 2,6-di-isopropylaniline overnight in Et$_2$O resulted in the

---

(18) Chisholm, M. H.; Eilerts, N. W. *Chem. Commun.* **1996**, 853−854.

(19) Chivers, T.; Fedorchuk, C.; Parvez, M. *Organometallics* **2005**, *24*, 580−586.

(20) Marshall, E. L.; Gibson, V. C.; Rzepa, H. S. *J. Am. Chem. Soc.* **2005**, *127*, 6048−6051.

(21) Chisholm, M. H.; Gallucci, J.; Phomphrai, K. *Inorg. Chem.* **2004**, *43*, 6717−6725.

(22) Chisholm, M. H.; Gallucci, J.; Phomphrai, K. *Chem. Commun.* **2003**, 48−49.

(23) Westerhausen, M.; Schneiderbauer, S.; Kneifel, A. N.; Söltl, Y.; Mayer, P.; Nöth, H.; Zhong, Z.; Dijkstra, P. J.; Feijen, J. *Eur. J. Inorg. Chem.* **2003**, 3432−3439.

(24) Dove, A. P.; Gibson, V. C.; Marshall, E. L.; White, A. J. P.; Williams, D. J. *Chem. Commun.* **2001**, 283−284.

(25) Aubrecht, K. B.; Hillmyer, M. A.; Tolman, W. B. *Macromolecules*, **2002**, *35*, 644−650.

(26) Dove, A. P.; Gibson, V. C.; Marshall, E. L.; Rzepa, H. S.; White, A. J. P.; Williams, D. J. *J. Am. Chem. Soc.* **2006**, *128*, 9834−9843.

(27) Nimitsiriwat, N.; Marshall, E. L.; Gibson, V. C.; Elsegood, M. R. J.; Dale, S. H. *J. Am. Chem. Soc.* **2004**, *126*, 13598−13599.

(28) Gibson, V. C.; Marshall, E. L.; Navarro-Llobet, D.; White, A. J. P.; Williams, D. J. *Dalton Trans.* **2003**, 4321−4322.

(29) Dove, A. P.; Gibson, V. C.; Marshall, E. L.; White, A. J. P.; Williams, D. J. *Chem. Commun.* **2002**, 1208−1209.

(30) Cheng, M.; Lobkovsky, E. B.; Coates, G. W. *J. Am. Chem. Soc.* **1998**, *120*, 11018−11019.

(31) Cheng, M.; Moore, D. R.; Reczek, J. J.; Chamberlain, B. M.; Lobkovsky, E. B.; Coates, G. W. *J. Am. Chem. Soc.* **2001**, *123*, 8738−8749.

(32) Moore, D. R.; Cheng, M.; Lobkovsky, E. B.; Coates, G. W. *Angew. Chem., Int. Ed.* **2002**, *41*, 2599−2602.

(33) Allen, S. D.; Moore, D. R.; Lobkovsky, E. B.; Coates, G. W. *J. Am. Chem. Soc.* **2002**, *124*, 14284−14285.

(34) Moore, D. R.; Cheng, M.; Lobkovsky, E. B.; Coates, G. W. *J. Am. Chem. Soc.* **2003**, *125*, 11911−11924.

(35) Byrne, C. M.; Allen, S. D.; Lobkovsky, E. B.; Coates, G. W. *J. Am. Chem. Soc.* **2004**, *126*, 11404−11405.

(36) Cheng, M.; Darling, N. A.; Lobkovsky, E. B.; Coates, G. W. *Chem. Commun.* **2000**, 2007−2008.

(37) Coates, G. W.; Moore, D. R. *Angew. Chem., Int. Ed.* **2004**, *43*, 6618−6639.

(38) Nozaki, K.; Nakano, K.; Hiyama, T. *J. Am. Chem. Soc.* **1999**, *121*, 11008−11009.

(39) Nakano, K.; Nozaki, K.; Hiyama, T. *J. Am. Chem. Soc.* **2003**, *125*, 5501−5510.

(40) Darensbourg, D. J.; Rainey, P.; Yarbrough, J. *Inorg. Chem.* **2001**, *40*, 986−993.

(41) Darensbourg, D. J.; Wildeson, J. R.; Yarbrough, J. C. *Organometallics* **2001**, *20*, 4413−4417.

(42) Chisholm, M. H.; Gallucci, J. C.; Zhen, H. H.; Huffman, J. C. *Inorg. Chem.* **2001**, *40*, 5051−5054.

(43) Eberhardt, R.; Allmendinger, M.; Luinstra, G. A.; Reiger, B. *Organometallics* **2003**, *22*, 211−214.

(44) Kim, I.; Kim, S. M.; Ha, C. S.; Park, D. W. *Macromol. Rapid Commun.* **2004**, *25*, 888−893.

(45) Herrmann, J. S.; Luinstra, G. A.; Roesky, P. W. *J. Organomet. Chem.* **2004**, *689*, 2720−2725.

(46) Lee, B. Y.; Kwon, H. Y.; Lee, S. Y.; Na, S. J.; Han, S.; Yun, H.; Lee, H.; Park, Y. W. *J. Am. Chem. Soc.* **2005**, *127*, 3031−3037.

(47) Xiao, Y.; Weng, Z.; Ding, K. *Chem.—Eur. J.* **2005**, *11*, 3668−3678.

(48) Xiao, Y.; Weng, Z.; Ding, K. *Macromolecules* **2006**, *39*, 128−137.

(49) Bourget-Merle, L.; Lappert, M. F.; Severn, J. R. *Chem. Rev.* **2002**, *102*, 3031−3066.

(50) Calligarir, M.; Randaccio, L. In *Comprehensive Coordination Chemistry*; Wilkinson, G., Gillard, R. D. McCleverty, J. Eds.; Pergamon Press Ltd: Oxford, 1987; Vol. 2, pp 723−726.

(51) Roesky, P. W. *Chem. Soc. Rev.* **2000**, 335−346.

(52) Barker, J.; Kilner, M. *Coord. Chem. Rev.* **1994**, *133*, 219−300.

(53) Edelmann, F. T. *Coord. Chem. Rev.* **1994**, *137*, 403−481.

(54) Schmidt, J. A. R.; Arnold, J. *Dalton Trans.* **2002**, 2890−2899.

(55) Schmidt, J. A. R.; Arnold, J. *Dalton Trans.* **2002**, 3454−3461.

(56) Schmidt, J. A. R.; Arnold, J. *Chem. Commun.* **1999**, 2149−2150.

(57) Schmidt, J. A. R.; Arnold, J. *Organometallics* **2002**, *21*, 2306−2313.

(58) Jenkins, H. A.; Abeysekera, D.; Dickie, D. A.; Clyburne, J. A. C. *Dalton Trans.* **2002**, 3919−3922.

(59) Boeré, R. T.; Cole, M. L.; Junk, P. C. *New J. Chem.* **2005**, *29*, 128−134.

(60) Cole, M. L.; Davies, A. J.; Jones, C.; Junk, P. C. *J. Organomet. Chem.* **2004**, *689*, 3093−3107.

(61) Bambirra, S.; Bouwkamp, M. W.; Meetsma, A.; Hessen, B. *J. Am. Chem. Soc.* **2004**, *126*, 9182−9183.

(62) Boeré, R. T.; Klassen, V.; Wolmershäusen, G. *J. Chem. Soc., Dalton Trans.* **1998**, 4147−4154.

(63) Xia, A.; El-Kaderi, H. M.; Heeg, M. J.; Winter, C. H. *J. Organomet. Chem.* **2003**, *682*, 224−232.

(64) Chan, N.; Barra, M.; Lee, I.; Chahal, N. *J. Org. Chem.* **2002**, *67*, 2271−2277.

(65) Dagorne, S.; Guzei, I. A.; Coles, M. P.; Jordan, R. F. *J. Am. Chem. Soc.* **2000**, *122*, 274−289.

(66) Vrieze, K.; van Koten, G. In *Comprehensive Coordination Chemistry*; Wilkinson, G., Gillard, R. D. McCleverty, J. Eds.; Pergamon Press: Elmsford, NY, 1987; Vol. 2, pp 195−206.

(67) Gantzel, P.; Walsh, P. J. *Inorg. Chem.* **1998**, *37*, 3450−3451.

(68) Hartman, W. W.; Dickey, J. B. *Org. Synth.* **1943**, *2*, 163−165.

Scheme 3. Postulated Solution State Isomers of *N*,*N*′-Bis(2,6-di-isopropylphenyl)triazene, L^1H

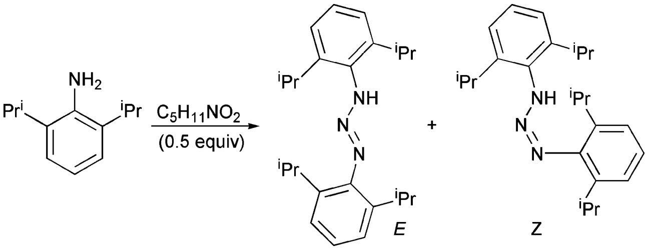

Scheme 4

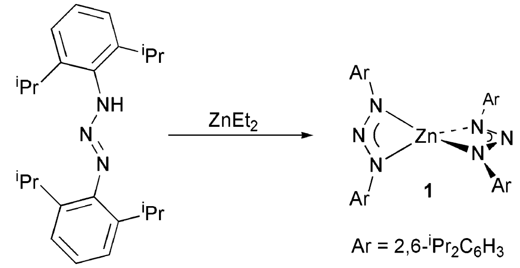

Scheme 5

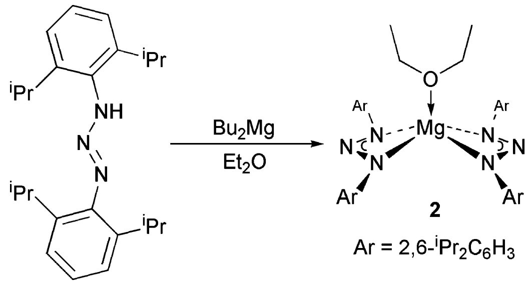

isolation of the triazene in 60% yield following recrystallization from nitromethane. ^1H NMR spectroscopy revealed the triazene to exist in solution as a mixture of isomers, in a ratio of ca. 7:1, with the major component believed to be the *E* isomer on steric grounds[64] and by comparison to the analogous acetamidine.[62]

All of our attempts to form mono-chelate zinc and magnesium alkyls led to the isolation instead of the respective bis(triazenide) complexes. Thus, the room temperature reaction of L^1H with $ZnEt_2$ in toluene resulted in the formation of $(L^1)_2Zn$, **1** (Scheme 4), even if an excess of $ZnEt_2$ was used (3.0 equiv). Similar attempts to produce a mono(triazenide) magnesium alkyl complex from the reaction of L^1H with $^{n/s}Bu_2Mg$ in Et_2O afforded a five-coordinate etherate, $[N(NAr)_2]_2Mg(Et_2O)$, **2** (Scheme 5), the solvent remaining intact even after recrystallization from heptane. We note that Walsh and co-workers[70] have previously synthesized a six-coordinate counterpart, $[N(N\text{-}p\text{-tolyl})_2]_2Mg(THF)_2$, the lower bulk of the *p*-tolyl groups allowing two solvent molecules to bind to the metal.

Crystals of **1** suitable for X-ray diffraction studies were obtained from a saturated pentane solution at room temperature (selected bond data are collated in Table 1). For reasons of clarity, the isopropyl substituents are not shown in Figure 1 (the complete structure may be viewed in Figure S1 within the Supporting Information). Although triazenide-1-oxide zinc complexes have been well studied, triazenide analogues are much less common,[71−73] and to the best of our knowledge, **1** is the first example of a structurally characterized zinc bis(triazenide) complex.

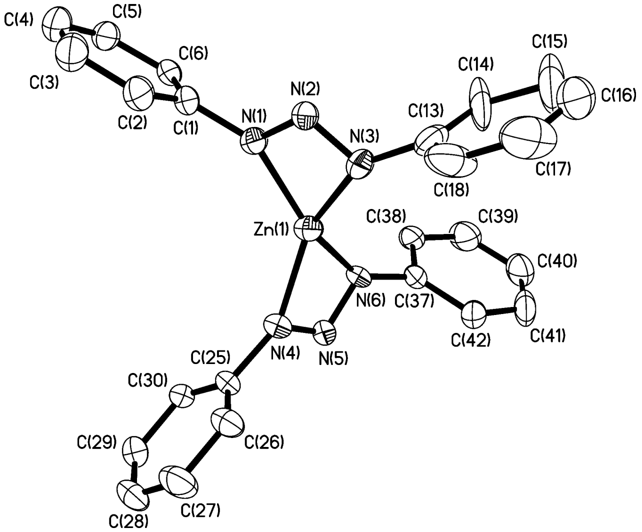

Figure 1. Molecular structure of **1** (50% probability ellipsoids). All of the isopropyl groups have been omitted for clarity.

Table 1. Selected Bond Lengths (Angstroms) and Angles (Degrees) for **1**

Zn(1)−N(1)	2.033(5)	Zn(1)−N(3)	2.068(5)
Zn(1)−N(4)	2.019(5)	Zn(1)−N(6)	2.089(5)
N(1)−N(2)	1.313(6)	N(2)−N(3)	1.321(7)
N(4)−N(5)	1.317(7)	N(5)−N(6)	1.302(6)
N(1)−Zn(1)−N(3)	62.30(19)	N(1)−Zn(1)−N(4)	132.61(19)
N(1)−Zn(1)−N(6)	149.11(19)	N(3)−Zn(1)−N(4)	145.5(2)
N(3)−Zn(1)−N(6)	124.34(19)	N(4)−Zn(1)−N(6)	62.05(19)
N(1)−N(2)−N(3)	107.3(4)	N(4)−N(5)−N(6)	107.9(5)
Zn(1)−N(1)−C(1)	147.6(4)	Zn(1)−N(3)−C(13)	147.4(4)
Zn(1)−N(4)−C(25)	146.3(4)	Zn(1)−N(6)−C(37)	146.6(4)

The zinc atom in **1** is distorted severely from an idealized tetrahedral geometry due to the acute chelate angle of the triazenide, with angles at the metal ranging from 62.05(19) [N(4)−Zn(1)−N(6)] to 149.11(19)° [N(1)−Zn(1)−N(6)]. The molecular structure shares many of the gross features previously described for a zinc bis(benzamidinate), $[\{PhC(NSiMe_3)_2\}_2Zn]$,[74] and two zinc bis(guanidinate)s $[\{(Me_3Si)_2NC(NR)_2\}_2Zn]$ ($R = {}^iPr$, Cy).[75] Both N_3Zn units approach planarity [to within 0.064 and 0.119 Å for the N(2) and N(5)-containing ligands respectively], with the angle between the two planes ca. 65.3°. The Zn−N bond lengths fall within a narrow range [2.019(5)−2.089(5) Å], and the anionic charges

---

(69) Hill, D. T.; Stanley, K. J.; Williams, J. E. K. K.; Love, B.; Fowler, P. J.; McCafferty, J. P.; Macko, E.; Berkoff, C. E.; Ladd, C. B. *J. Med. Chem.* **1983**, *26*, 865−869.

(70) Westhusin, S.; Gantzel, P.; Walsh, P. J. *Inorg. Chem.* **1998**, *37*, 5956−5959.

(71) Brinckman, F. E.; Haiss, H. S.; Robb, R. A. *Inorg. Chem.* **1964**, *4*, 936−942.

(72) Corbett, M.; Hoskins, B. F. *Inorg. Nucl. Chem. Lett.* **1970**, *6*, 261−264.

(73) Friederichs, N. H.; Ijpeij, E. G.; Mueller, A. G.; Schottenberger, H.; Wang, B.; Wurst, K. WO 2004003030.

(74) Buijink, J. K.; Noltemeyer, M.; Edelmann, F. T. *Z. Naturforsch., B* **1991**, *46*, 1328−1332.

(75) Coles, M. P.; Hitchcock, P. B. *Eur. J. Inorg. Chem.* **2004**, 2662−2672.

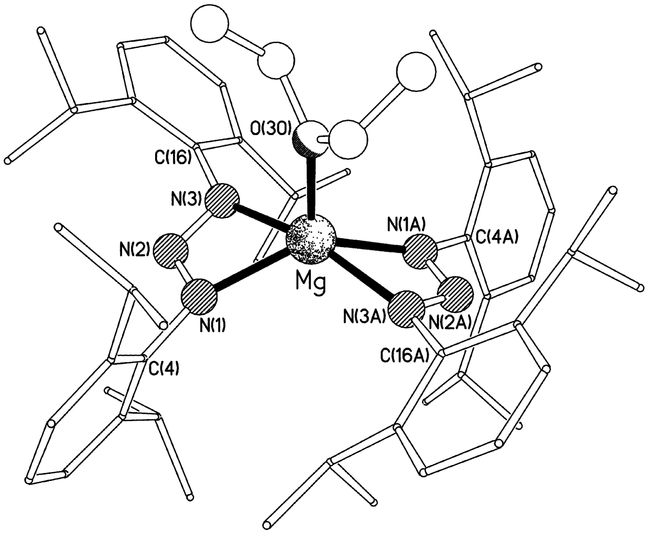

Figure 2. Molecular structure of the C_2-symmetric **2**.

Table 2. Selected Bond Lengths (Angstroms) and Angles (Degrees) for **2**

Mg−N(1)	2.1174(12)	Mg−N(3)	2.1568(12)
Mg−O(30)	2.0545(18)	Mg−N(1A)	2.1174(12)
Mg−N(3A)	2.1568(12)	N(1)−N(2)	1.3105(17)
N(2)−N(3)	1.3045(16)		
N(1)−Mg−N(3)	60.22(5)	N(1)−Mg−O(30)	110.98(4)
N(1)−Mg−N(1A)	138.03(8)	N(1)−Mg−N(3A)	113.26(5)
N(3)−Mg−O(30)	98.17(4)	N(3)−Mg−N(1A)	113.26(5)
N(3)−Mg−N(3A)	163.66(8)	O(30)−Mg−N(1A)	110.98(4)
O(30)−Mg−N(3A)	98.17(4)	N(1A)−Mg−N(3A)	60.22(5)
N(1)−N(2)−N(3)	110.20(12)	Mg−N(1)−C(4)	151.74(10)
Mg−N(3)−C(16)	149.52(10)	N(2)−N(1)−C(4)	112.66(12)
N(2)−N(3)−C(16)	115.61(12)		

of both triazenide ligands are delocalized over the N_3 backbones with four similar N−N bond lengths observed [N(1)−N(2) = 1.313(6), N(2)−N(3) = 1.321(7), N(4)−N(5) = 1.317(7), N(5)−N(6) = 1.302(6) Å].

Diffraction quality crystals of **2** were isolated from a saturated heptane solution at room temperature; the molecular structure is shown in Figure 2, and selected bond parameters are listed in Table 2. The five-coordinate metal adopts a highly distorted square-pyramidal geometry with the magnesium displaced by ca. 0.53 Å in the direction of the etherate oxygen from the best-fit plane through N(1), N(3), N(1A), and N(3A) (the four basal nitrogen atoms being coplanar to ca. 0.23 Å). Angles between the oxygen atom and the four-coordinated nitrogens range from 98.17(4) to 110.98(4)°. The triazenide fragments exhibit unremarkable bond distances and angles, with the N−N backbone bond lengths [1.3045(16)−1.3105(17) Å] and the chelate bite angle [N(1)−Mg−N(3) = 60.22(5)°] being comparable to those observed in the structure of **1**.

Syntheses of Acetamidinate Complexes. The inability of the triazenide ligand to stabilize mono-chelates renders it an unsuitable support for divalent magnesium- and zinc-based single-site catalysts. To determine how large the ancillary ligand must be to suppress bis-chelation, we next examined the acetamidinate ligand L^2. Although the direct comparison of triazenide and amidinate ligands has, to the best of our knowledge, not been investigated previously in this manner, several studies have highlighted the importance of the substituent on the central carbon atom of amidinate ligands: as this group increases in size, so the *N*-substituents are increasingly repelled, leading to heightened steric protection of the metal center. We therefore anticipated that the acetamidinate ligand L^2 would afford greater steric protection to metals than the triazenide L^1, and the chances of obtaining mono-chelate species would be improved.

Scheme 6. Selected Literature Examples of Structurally Characterized Zinc Amidinate Complexes

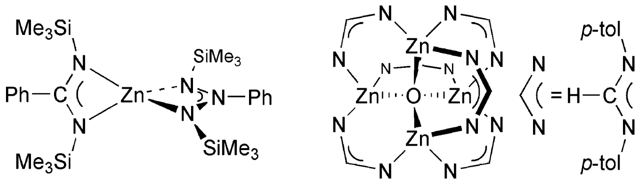

Although amidines have been extensively employed as ancillary ligands in transition metal, lanthanide, and main-group metal complexation chemistry, only a relatively small number of amidinate complexes of zinc(II) and magnesium(II) have been reported. The known amidinate zinc(II) complexes are either bis-chelates[53,76] or oxygenated tetranuclear zinc aggregates[77,78] (Scheme 6). By contrast, several mono-chelated amidinate magnesium(II) complexes have been synthesized previously, including [ArC(N^{i}Pr)$_2$]MgI(THF)$_2$ (Ar = 2,6-(4-^{t}Bu-C$_6$H$_4$)$_2$C$_6$H$_3$),[54] [^{t}BuC(NAr)$_2$]MgCp(THF)$_n$ (Ar = 2,6-^{i}Pr$_2$C$_6$H$_3$, n = 0 and Ar = 2,4,6-Me$_3$C$_6$H$_2$, n = 1)[63] and [^{n}BuC(NCy)$_2$]Mg{η^1-N(Ar)P-^{n}BuPh}(Et$_2$O) (Ar = 2,6-^{i}Pr$_2$C$_6$H$_3$)[79] and the formamidinates [{HC(NPh)$_2$Mg(THF)}$_2$(μ-Cl)$_2$(μ-THF)][80] and [{HC(NAr)$_2$}Mg(μ-Cl)(THF)]$_2$ (Ar = 2,6-^{i}Pr$_2$C$_6$H$_3$),[81] although bis-chelate counterparts are again more common.[53,54,59,63,82−86]

Despite the expected increase in steric protection, all of our attempts to isolate mono-chelated zinc(II) and magnesium(II) complexes of L^2 were unsuccessful; instead the major components of all of the product mixtures were the bis(amidinate) complexes $(L^2)_2Zn$, **3**, and $(L^2)_2Mg$, **4**. For example, lithiation of L^2H and the subsequent addition to $ZnCl_2$ in toluene, or the direct reaction of L^2H with

---

(76) Buijink, J. K.; Noltemeyer, M.; Edelmann, F. T. *Z. Naturforsch.* **1991**, *46*, 1328−1332.

(77) Cotton, F. A.; Daniels, L. M.; Falvello, L. R.; Matonic, J. H.; Murillo, C. A.; Wang, X.; Zhou, H. *Inorg. Chim. Acta* **1997**, *266*, 91−102.

(78) Cole, M. L.; Evans, D. J.; Junk, P. C.; Louis, L. M. *New J. Chem.* **2002**, *26*, 1015−1024.

(79) Chivers, T.; Copsey, M. C.; Fedorchuk, C.; Parvez, M.; Stubbs, M. *Organometallics* **2005**, *24*, 1919−1928.

(80) Cotton, F. A.; Haefner, S. C.; Matonic, J. H.; Wang, X.; Murillo, C. A. *Polyhedron* **1997**, *16*, 541−550.

(81) Andrews, P. C.; Brym, M.; Jones, C.; Junk, P. C.; Kloth, M. *Inorg. Chim. Acta* **2006**, *359*, 355−363.

(82) Westerhausen, M.; Hausen, H. D. *Z. Anorg. Allg. Chem.* **1992**, *615*, 27−34.

(83) Srinivas, B.; Chang, C. C.; Chen, C. H.; Chiang, M. Y.; Chen, I.-T.; Wang, Y.; Lee, G.-H. *J. Chem. Soc., Dalton Trans.* **1997**, 957−963.

(84) Sadique, A. R.; Heeg, M. J.; Winter, C. H. *Inorg. Chem.* **2001**, *40*, 6349−6355.

(85) Kincaid, K.; Gerlach, C. P.; Giesbrecht, G. R.; Hagadorn, J. R.; Whitener, G. D.; Shafir, A.; Arnold, J. *Organometallics* **1999**, *18*, 5360−5366.

(86) Walther, D.; Gebhardt, P.; Fischer, R.; Kreher, U.; Görls, H. *Inorg. Chim. Acta* **1998**, *281*, 181−189.

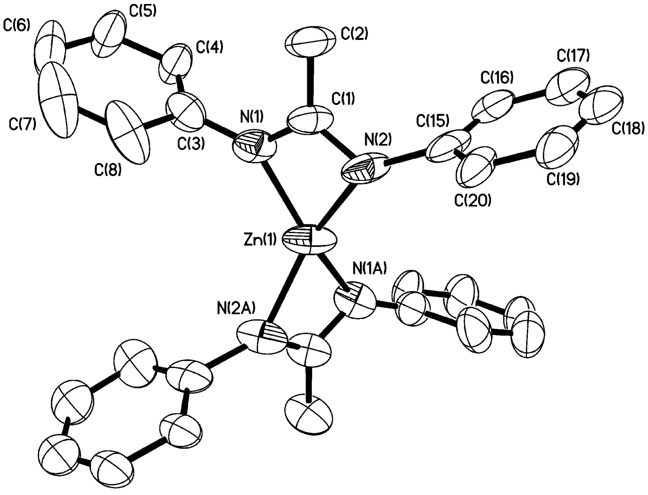

Figure 3. Molecular structure of **3** (50% probability ellipsoids). All of the isopropyl groups have been omitted for clarity.

Table 3. Selected Bond Lengths (Angstroms) and Angles (Degrees) for **3**

Zn(1)−N(1)	2.031(5)	Zn(1)−N(2)	2.038(4)
N(1)−C(1)	1.328(7)	N(2)−C(1)	1.325(7)
C(1)−C(2)	1.499(7)		
N(1)−Zn(1)−N(2)	65.86(18)	N(1)−Zn(1)−N(1A)	148.2(2)
N(1)−Zn(1)−N(2A)	124.2(2)	N(1)−C(1)−N(2)	113.0(4)
N(2)−Zn(1)−N(2A)	147.5(3)	Zn(1)−N(2)−C(1)	90.4(3)
Zn(1)−N(1)−C(1)	90.7(3)	Zn(1)−N(2)−C(15)	141.8(7)
Zn(1)−N(1)−C(3)	144.8(4)	N(2)−C(1)−C(2)	123.1(5)
N(1)−C(1)−C(2)	123.8(5)	C(1)−N(2)−C(15)	123.4(8)
C(1)−N(1)−C(3)	123.1(5)	Zn(1)···C(1)···C(2)	179.4(5)
C(1)···Zn(1)···C(1A)	179.5(3)		

$Zn[N(SiMe_3)_2]_2$, resulted in a mixture of **3** and the appropriate mono-chelated zinc(II) halide or amide complex, and attempts to recrystallize these species repeatedly led to the fractional precipitation of **3**. Similarly, the reaction of L^2H and ^iPrMgCl in toluene afforded **4**, with a minor component of the crude product mixture tentatively assigned as the desired mono-chelate $(L^2)MgCl$ on the basis of ^1H NMR spectroscopy.

Crystals of **3** were grown by slow cooling of a heptane solution from 60 °C to room temperature. As shown in Figure 3, complex **3** is structurally similar to **1** with the two L^1 ligands coordinated in a chelating η^2-fashion, affording a distorted tetrahedral geometry about the zinc atom (angles at the metal ranging from 65.86(18) to 148.2(2)°, Table 3) (the positions of the isopropyl substituents may be viewed in Figure S3). The four atoms in each ZnN_2C unit are perfectly planar, and the mean Zn−N bond distance (2.035 Å) is similar to that observed in the structure of **1** (2.052 Å). As in the bis(triazenide) counterpart, the monoanionic charge is delocalized over the amidinate NCN backbones, as shown by the near-identical C(1)−N(1) and C(1)−N(2) bond distances [1.325(7) and 1.328(7) Å].

The solid-state structure of the magnesium counterpart **4** revealed the presence of two crystallographically independent molecules (**4-I** and **4-II**) with essentially identical geometries (Figure 4 and Table 4 in this paper and Figures S4−S7 in the Supporting Information). The bond angles at magnesium range from 65.35(15) to 151.56(17)° for molecule **4-I** [65.97(16) to 151.35(18)° for molecule **4-II**], with considerable distortion from tetrahedral coordination attributed to the minimization of steric clashes between the *N*-aryl substituents. The magnesium atom lies in the planes of both NCN ligand cores to within 0.04 Å for molecule **4-I** [0.03 Å for **4-II**], and both C(2) and C(32) exhibit sp^2 trigonal planar geometries; the two NCN planes are inclined by ca. 54° for **4-I**, and ca. 55° for **4-II**. Delocalization of the anionic charge over the NCN amidinate backbones results in similar bond lengths for N(1)−C(2) and C(2)−N(3) [1.328(6), 1.321(6) for **4-I**; 1.322(6) and 1.327(6) Å for **4-II**], and for N(31)−C(32) and C(32)−N(33) [1.317(5), 1.342(6) for **4-I**; 1.334(6), 1.323(6) Å for **4-II**]. The four Mg−N bond lengths fall within a narrow range of 2.039(4)−2.046(4) for **4-I** [2.039(4)−2.059(4) Å for **4-II**], and the chelate rings have acute N−Mg−N angles [N(1)−Mg−N(3) = 65.35(15) and N(31)−Mg−N(33) = 65.78(15) for **4-I**; 65.97(16) and 66.07(16)° respectively for molecule **4-II**], consistent with values previously reported for other bis(amidinate) magnesium complexes.[53,54,63,82−86]

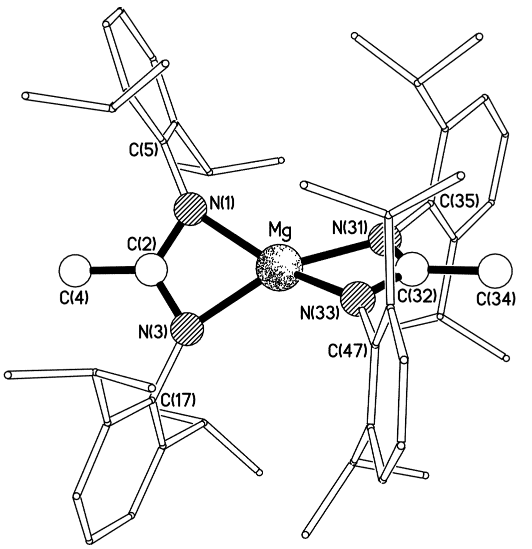

Figure 4. Molecular structure of one (**I**) of the two independent complexes present in the crystals of **4**.

We have also found that the reaction of L^2H with excess quantities of freshly purchased solutions of $ZnMe_2$ or $ZnEt_2$ leads to the clean formation of **3**. However, when older batches of the dialkylzinc reagents were used, alternative products were obtained, containing both amidinate and alkyl ligands in a 1:2 ratio (^1H NMR). The eventual formulation of these products as $\{(L^2)Zn_2R_2\}_2O$ (R = Me, **5**; R = Et, **6**) was facilitated by X-ray crystallographic analyses. As these two compounds are approximately isostructural, only the structure of **5** is described here (bond parameters and a full discussion of the molecular structure of **6** may be found in the Supporting Information). Both complexes are composed of a four-coordinate central oxygen ion surrounded solely by a tetrahedral arrangement of zinc centers (Figure 5). Each metal atom bears a single alkyl ligand, and both amidinate ligands bind two zinc ions in a $\mu-\eta^1:\eta^1$ bridging mode. We have not attempted to identify either the precise conditions required for the syntheses of **5** or **6** or the source of the oxygen atom. We do, however, note that the sensitivity of amidinate zinc complexes to moisture (and the oxophilic

Table 4. Selected Bond Lengths (Angstroms) and Angles (Degrees) for Both Independent Complexes (**4-I** and **4-II**) Present in the Crystals of **4**

	4-I	**4-II**		**4-I**	**4-II**
Mg−N(1)	2.046(4)	2.044(4)	Mg−N(3)	2.046(4)	2.054(4)
Mg−N(31)	2.039(4)	2.059(4)	Mg−N(33)	2.043(4)	2.039(4)
N(1)−C(2)	1.328(6)	1.322(6)	C(2)−N(3)	1.321(6)	1.327(6)
C(2)−C(4)	1.490(6)	1.508(7)	N(31)−C(32)	1.317(5)	1.334(6)
C(32)−N(33)	1.342(6)	1.323(6)	C(32)−C(34)	1.482(6)	1.509(6)
N(1)−Mg−N(3)	65.35(15)	65.97(16)	N(1)−Mg−N(31)	123.71(16)	122.73(18)
N(1)−Mg−N(33)	151.56(17)	151.35(18)	N(3)−Mg−N(31)	151.35(17)	150.5(2)
N(3)−Mg−N(33)	120.96(16)	121.61(18)	N(31)−Mg−N(33)	65.78(15)	66.07(16)
N(1)−C(2)−N(3)	113.1(4)	114.7(4)	N(1)−C(2)−C(4)	123.4(4)	123.0(4)
Mg−N(1)−C(2)	90.7(2)	89.9(3)	Mg−N(3)−C(2)	90.9(3)	89.4(3)
Mg−N(31)−C(32)	91.1(3)	89.1(3)	Mg−N(33)−C(32)	90.2(2)	90.3(3)
N(3)−C(2)−C(4)	123.5(4)	122.3(4)	N(31)−C(32)−N(33)	112.9(4)	114.5(4)
N(31)−C(32)−C(34)	123.7(4)	121.7(4)	N(33)−C(32)−C(34)	123.3(4)	123.8(4)
Mg−N(1)−C(5)	147.3(3)	147.4(3)	Mg−N(3)−C(17)	147.0(3)	148.3(4)
Mg−N(31)−C(35)	147.6(3)	148.1(4)	Mg−N(33)−C(47)	146.7(3)	146.5(3)
C(2)−N(1)−C(5)	121.8(4)	122.3(4)	C(2)−N(3)−C(17)	121.7(4)	121.6(4)
C(32)−N(31)−C(35)	121.2(4)	122.2(4)	C(32)−N(33)−C(47)	122.4(4)	122.5(4)

nature of zinc clusters[78]) has been previously documented in reports concerning the formation of tetranuclear zinc clusters of the type shown in Scheme 6.

In **5** (Figures 5 and S8 in the Supporting Information), the bridging oxygen adopts a distorted tetrahedral geometry with the angles made by its bonds to the four zinc atoms ranging from 102.43(6) to 112.68(7)° (Table 5). Each zinc center exhibits a distorted trigonal-planar conformation, with the N−Zn−C angles significantly wider than the N−Zn−O angles (ca. 130 and 108°, respectively). The six atoms of both of the Zn_2N_2CO rings are planar to within 0.061 [Zn(1), Zn(2)] and 0.085 Å [Zn(3), Zn(4)]. The bond lengths of C(1)−N(1) and C(1)−N(2) are the same (ca. 1.33 Å), indicating that the anionic charge is again delocalized over the ligand backbone. The four Zn−O bond lengths are also essentially the same (ca. 1.95 Å) and are similar to those of $[HC(NPh)_2]_6Zn_4O$,[77] $[HC(N\text{-}p\text{-}CH_3C_6H_4)_2]_6Zn_4O$,[78] and the triazenide complex $[N(NPh)_2]_6Zn_4O$.[72]

Table 5. Selected Bond Lengths (Angstroms) and Angles (Degrees) for **5**

Zn(1)−N(1)	1.9625(17)	Zn(2)−N(2)	1.9743(18)
Zn(3)−N(3)	1.9672(17)	Zn(4)−N(4)	1.9731(16)
Zn(1)−O(1)	1.9500(14)	Zn(2)−O(1)	1.9510(14)
Zn(3)−O(1)	1.9489(13)	Zn(4)−O(1)	1.9531(14)
N(1)−C(1)	1.333(2)	N(2)−C(1)	1.332(3)
N(3)−C(27)	1.332(2)	N(4)−C(27)	1.334(2)
Zn(1)−C(53)	1.956(3)	Zn(2)−C(54)	1.959(3)
Zn(3)−C(55)	1.958(3)	Zn(4)−C(56)	1.956(2)
Zn(1)−O(1)−Zn(2)	112.68(7)	Zn(1)−O(1)−Zn(3)	102.43(6)
Zn(1)−O(1)−Zn(4)	110.87(7)	Zn(2)−O(1)−Zn(3)	110.02(7)
Zn(2)−O(1)−Zn(4)	108.58(7)	Zn(3)−O(1)−Zn(4)	112.21(7)
N(1)−Zn(1)−O(1)	110.43(6)	N(2)−Zn(2)−O(1)	109.32(6)
N(3)−Zn(3)−O(1)	110.58(6)	N(4)−Zn(4)−O(1)	109.49(6)
N(1)−Zn(1)−C(53)	128.53(10)	N(2)−Zn(2)−C(54)	129.04(11)
N(3)−Zn(3)−C(55)	129.93(10)	N(4)−Zn(4)−C(56)	130.80(10)
N(1)−C(1)−N(2)	120.87(18)	N(3)−C(27)−N(4)	120.84(18)
C(53)−Zn(1)−O(1)	120.97(10)	C(54)−Zn(2)−O(1)	121.61(11)
C(55)−Zn(3)−O(1)	119.42(10)	C(56)−Zn(4)−O(1)	119.68(10)
N(1)−C(1)−C(2)	119.71(17)	N(2)−C(1)−C(2)	119.41(17)
N(3)−C(27)−C(28)	119.95(17)	N(4)−C(27)−C(28)	119.21(17)
C(1)−N(1)−C(3)	118.60(17)	C(1)−N(2)−C(15)	118.32(17)
C(27)−N(3)−C(29)	119.31(16)	C(27)−N(4)−C(41)	117.77(16)

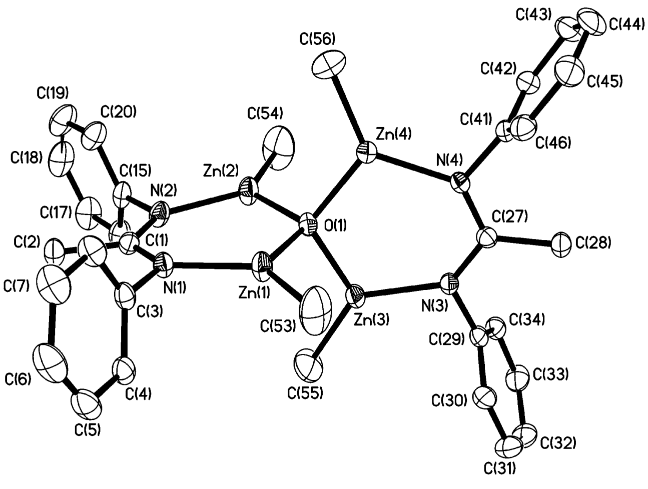

Figure 5. Molecular structure of **5** (50% probability ellipsoids). All of the isopropyl groups have been omitted for clarity (see also Figure S8).

Synthesis of *tert*-Butylamidinate Complexes. As observed for L^1, the acetamidinate ligand L^2 evidently possesses insufficient bulk to act as a suitable ancillary ligand for single-site zinc or magnesium-based catalysts. In the final phase of this study, we therefore increased the steric protection further by switching our attention to the *t*-butylamidinate analogue L^3.[63] In contrast with the behavior described above, lithiation of L^3H followed by reaction with $ZnCl_2$ in THF yielded $(L^3)ZnCl(THF)$, **7**. Recrystallization from toluene resulted in the loss of the coordinated solvent to form the chloro-bridged dimeric species, $[(L^3)Zn(\mu\text{-}Cl)]_2$, **8**. In addition, $(L^3)ZnN(SiMe_3)_2$, **9**, can be prepared from the reaction of **8** with $KN(SiMe_3)_2$. Side-formation of the bis(chelate) $(L^3)_2Zn$ was not observed in any of these reactions, and **7**−**9** are the first reported examples of mono-(η^2-amidinate) zinc(II) complexes (Scheme 7).

Crystals of **8** suitable for X-ray diffraction were grown by allowing a saturated toluene solution to stand at room temperature. Crystallographic analysis revealed that this complex exists as a chloride-bridged dimer in the solid state (Figure 6), with the two halves of the molecule being related by a center of inversion. The central Zn_2Cl_2 core is coplanar and is slightly asymmetric, with each zinc having one Zn−Cl interaction slightly longer than the other [Zn(1)−Cl(1A) = 2.2928(4), Zn(1)−Cl(1) = 2.3120(5) Å, Table 6]. Both of the zinc atoms are coplanar to within 0.026 Å of the amidinate NCN planes, which are orientated in an approximately orthogonal fashion to the central Zn_2Cl_2 core.

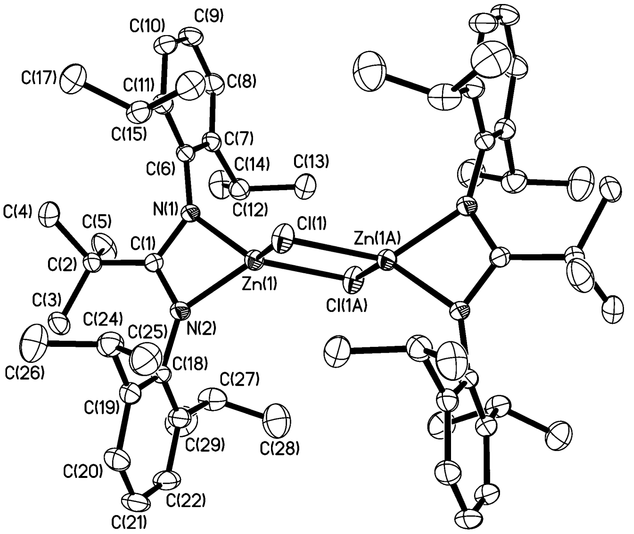

Figure 6. Centrosymmetric molecular structure of **8** (50% probability ellipsoids).

Scheme 7. Synthesis of **7**−**9**[a]

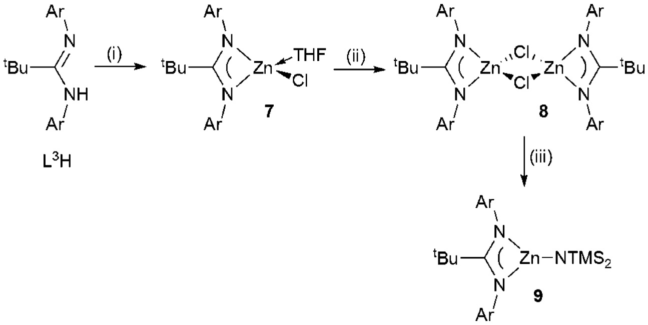

[a] (i) ^{n}BuLi, $ZnCl_2$, THF; (ii) recrystallize from toluene; (iii) $KN(SiMe_3)_2$.

Table 6. Selected Bond Lengths (Angstroms) and Angles (Degrees) for **8**

Zn(1)−N(1)	1.9973(12)	Zn(1)−N(2)	1.9984(12)
Zn(1)−Cl(1)	2.3120(5)	Zn(1)−Cl(1A)	2.2928(4)
C(1)−N(1)	1.3479(18)	C(1)−N(2)	1.3386(18)
C(1)−C(2)	1.540(2)		
N(1)−Zn(1)−N(2)	66.49(5)	N(1)−Zn(1)−Cl(1)	123.44(4)
N(1)−Zn(1)−Cl(1A)	127.34(4)	N(2)−Zn(1)−Cl(1)	122.23(4)
N(2)−Zn(1)−Cl(1A)	125.15(4)	Cl(1)−Zn(1)−Cl(1A)	94.552(16)
C(1)−N(1)−Zn(1)	92.01(9)	C(1)−N(2)−Zn(1)	92.25(9)
C(1)−N(1)−C(6)	132.74(12)	C(1)−N(2)−C(18)	133.40(13)
C(2)−C(1)−N(1)	124.24(13)	C(2)−C(1)−N(2)	126.51(13)
Zn(1)−N(1)−C(6)	135.24(10)	Zn(1)−N(2)−C(18)	134.22(10)

Opposing aryl rings thus adopt near-parallel orientations, thus minimizing steric interactions between the ^{i}Pr substituents: a similar conformation has been reported previously for the related β-diiminate complex, $[(HC\{C(Me)NAr\}_2)Zn(\mu\text{-}F)]_2$.[87]

Mono-chelate magnesium complexes have also been isolated using the *tert*-butylamidinate ligand. Thus, as outlined in Scheme 8, treatment of L^3Li with ^{i}PrMgCl in Et_2O or THF affords $(L^3)Mg^iPr(L)$, **10** (L = Et_2O) and **11** (L = THF). This observation contrasts with aspects of our previous work on magnesium β-diketiminate complexes, specifically the isolation of $[HC(CMeN\text{-}2,6\text{-}{}^iPr_2C_6H_3)_2]Mg^iPr$ as a solvent-free,[88] three-coordinate compound and reflects the smaller steric demands of the amidinate ligand family.

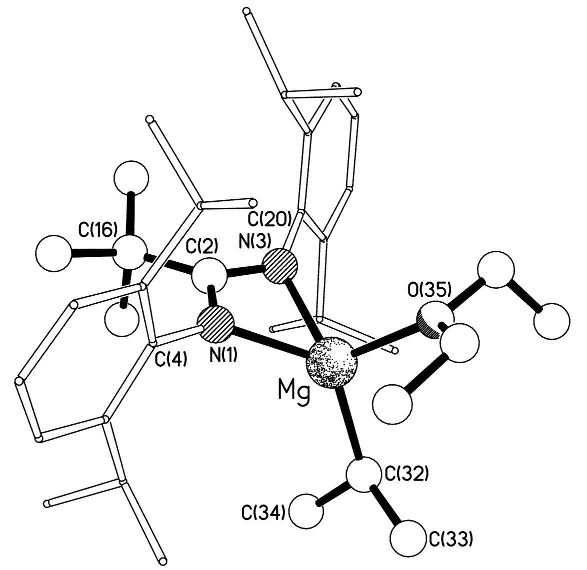

Figure 7. Molecular structure of **10**.

Scheme 8

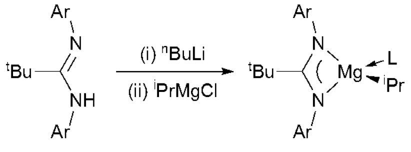

L = Et_2O, **10**;
L = THF, **11**

Table 7. Selected Bond Lengths (Angstroms) and Angles (Degrees) for **10**

Mg−N(1)	2.1089(14)	Mg−N(3)	2.0908(14)
Mg−C(32)	2.156(2)	Mg−O(35)	2.0740(16)
N(1)−C(2)	1.3425(18)	C(2)−N(3)	1.3399(19)
C(2)−C(16)	1.561(2)		
N(1)−Mg−N(3)	63.58(5)	N(1)−Mg−C(32)	128.70(8)
N(1)−Mg−O(35)	116.00(7)	N(3)−Mg−C(32)	127.13(8)
N(3)−Mg−O(35)	107.90(7)	C(32)−Mg−O(35)	107.16(9)
N(1)−C(2)−N(3)	111.13(12)	N(1)−C(2)−C(16)	124.13(13)
N(3)−C(2)−C(16)	123.38(12)	Mg−N(1)−C(2)	90.93(9)
Mg−N(3)−C(2)	91.79(9)	Mg−N(1)−C(4)	140.34(10)
Mg−N(3)−C(20)	138.64(11)	C(2)−N(1)−C(4)	128.37(12)
C(2)−N(3)−C(20)	129.57(13)		

Crystals of **10** suitable for X-ray diffraction were grown by allowing a saturated heptane solution to stand at room temperature for several days. As shown in Figure 7, **10** exists as a four-coordinate magnesium complex with one molecule of diethyl ether coordinated to the metal, affording a highly distorted tetrahedral geometry about the magnesium atom with the range of angles about magnesium being 63.58(5) to 128.70(8)° (Table 7). The core of the amidinate ligand is close to planar, with the sum of the angles around N(1), N(3), and C(2) being 359.64, 360.00, and 358.64°, respectively, and the magnesium atom lies ca. 0.54 Å out of the amidinate NCN chelate plane. Both Mg−N bond lengths [2.0908(14), 2.1089(14) Å] and the N(1)−Mg−N(3) angle [63.58(5)°] are comparable to those found in the solid-state structure of

---

(87) Hao, H.; Cui, C.; Roesky, H. W.; Bai, G.; Schmidt, H.-G.; Noltemeyer, M. *Chem. Commun.* **2001**, 1118−1119.

(88) Dove, A. P.; Gibson, V. C.; Marshall, E. L.; White, A. J. P.; Williams, D. J. *Dalton Trans.* **2004**, 570−578.

Table 8. M−N−C$_{ipso}$ Bond Angles (Degrees) for **1**−**4**, **8**, and **10**

complex	M−*N*-aryl C$_{ipso}$ bond angles
1, $[N(NAr)_2]Zn$	146.6(4), 146.3(4), 147.4(4), 147.6(4)
2, $[N(NAr)_2]Mg(Et_2O)$	151.74(10), 149.52(10)
3, $[MeC(NAr)_2]Zn$	141.8(7), 144.8(4)
4-I, $[MeC(NAr)_2]Mg$	147.3(3), 147.0(3), 147.6(3), 146.7(3)
4-II, $[MeC(NAr)_2]Mg$	147.4(3), 148.3(4), 148.1(4), 146.5(3)
8, $\{[^tBuC(NAr)_2]Zn(\mu\text{-}Cl)\}_2$	135.24(10), 134.22(10)
10, $[^tBuC(NAr)_2]Mg(^iPr)(Et_2O)$	140.34(10), 138.64(11)

Scheme 9

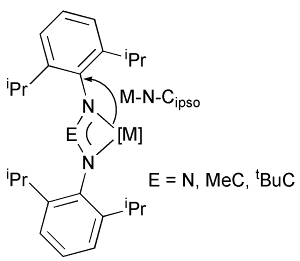

$(L^2)_2Mg$, **4**. However, the average C−N−C$_{ipso}$ angle of 128.97° is notably larger than that in **4** (122.05°), an effect attributed to the steric demand of the bulkier ^{t}Bu substituent on the central carbon of the NCN unit.

Comparison of the Steric Properties of the Three Ligands. Our results clearly show that, while the *tert*-butylamidinate ligand is capable of supporting magnesium and zinc mono-chelate derivative chemistry, the corresponding acetamidinate and triazenide are not. To quantify the steric protection afforded by each of these three ligands to a metal center, Table 8 summarizes the M−N−C$_{ipso}$ bond angles (Scheme 9) measured for **8** and **10**. With the caveat that the *N*-aryl substituents in the bis-chelates (i.e., **1**−**4**) will be subject to intramolecular ligand−ligand repulsions, the angles reported here are nonetheless consistent with the *N*-aryl rings being projected increasingly toward the metal, as the substituent upon the central atom of the triatomic ligand backbone becomes larger. For example, comparing data for the isostructural zinc bis-chelates **1** and **3** indicates that the central MeC unit in the ligand backbone of **3** reduces the Zn−N−C$_{ipso}$ angles by ca. 4° more than the corresponding triazenide ligand does (average angle = 147.0 for **1** and 143.3° for **3**; see Figures S12 and S13 in the Supporting Information for overlay diagrams). Although a direct comparison between **2** and **4** is complicated by the five-coordinate nature of the former, a similar effect is nonetheless observed (average Mg−N−C$_{ipso}$ angles: 150.6 for **2**; 147.2 for **4-I**; 147.6° for **4-II**). Consistently, the structures of the four-coordinate L^3 complexes **8** and **10** exhibit notably smaller angles (134.7 and 139.5°, respectively). These values compare well with structural data reported for $[RC(NR')_2]AlMe_2$ complexes, where the corresponding angles fall from ca. 144 to ca. 134°, on increasing the R group from methyl to *t*-butyl.[65] Although the difference between the M−N−C$_{ipso}$ angles for methyl versus *t*-butyl backbone substituents may seem relatively small, it is clear that it is sufficient to favor mono-chelation over bis-chelation, a crucial factor for stabilizing well-behaved molecular catalysts.

Conclusion

By studying three structurally related ligands, we have confirmed that suitable functionalization of the central carbon atom allows the steric bulk of an amidinate ligand to be finely adjusted to favor mono- over bis-chelation. Although the influence of the amidinate carbon substituent has been described in previous reports,[65] its role in preventing bis-chelate formation, a key factor in the design of amidinate-supported catalytic sites for polymerization chemistry, has not been fully appreciated prior to this work.

These studies further suggest that the 2,6-di-isopropylphenyl substituent is of insufficient size to allow the ready isolation of mono(triazenide) divalent metal complexes. Ligand L^1 will therefore probably be more suited to the stabilization of higher oxidation state metals. Indeed, we have previously disclosed that group 4 derivatives of the type $(L^1)_2MX_2$ (M = Ti, Zr[89]) act as olefin polymerization catalysts.[90]

Experimental Section

All manipulations of air- and/or moisture-sensitive compounds were performed under an atmosphere of dry nitrogen gas using standard high vacuum Schlenk and cannula techniques or in an inert atmosphere glovebox. NMR spectra were recorded on a Bruker DRX-400 spectrometer (^{1}H and ^{13}C at 400.129 and 100.613 MHz respectively). Elemental analyses were performed by the microanalytical services of the Chemistry Department of London Metropolitan University.

Heptane and toluene were dried by passing through a column of commercially available Q-5 catalyst (13% copper(I) oxide on Al_2O_3) and activated Al_2O_3 (pellets, 3 mm) under a stream of dry nitrogen gas and were then stored over a potassium mirror prior to use. THF and CH_2Cl_2 were distilled from potassium and CaH_2 respectively and stored over activated 3 Å molecular sieves. The amidines[62,63] were synthesized in accordance with literature procedures and all of the other reagents were used as supplied. Bu_2Mg is a commercially available reagent (Aldrich) containing equimolar quantities of *n*-butyl and *sec*-butyl alkyl groups.[91]

***N,N′*-Bis(2,6-di-isopropylphenyl)triazene, L^{1}H.** Isoamylnitrite (13.42 cm^3, 1.0×10^{-1} mol) was added over 90 min to a cooled (0 °C) solution of distilled 2,6-di-isopropylaniline (9.41 cm^3, 5.0×10^{-2} mol) in 100 cm^3 Et_2O. The reaction was then stirred at room temperature overnight (18 h). Volatiles were removed under reduced pressure at room temperature (the product is thermally sensitive) to afford an oil, which was dissolved in the minimum amount of nitromethane and chilled to −20 °C. The crystalline material thus obtained was filtered cold and washed successively with small quantities of cold nitromethane until it turned white. After drying in vacuo at 35 °C, 5.5 g (1.5×10^{-2} mol, 60%) product was obtained, which was stored at −20 °C. The compound exists as a 7:1 mixture of isomers. Anal. Calcd for $C_{24}H_{35}N_3$: C 78.85, H 9.65, N 11.49. Found C 79.07, H 9.40, N 11.53. ^{1}H NMR ($CDCl_3$): δ 9.15 (br s, 1H, N*H*) 7.26−7.03 (m, 4H, H_{meta}), 6.84 (d, 2H, H_{para}), 3.20 (m, 3.5 H, C*H*Me$_2$), 2.96 (m, 0.5H, C*H*Me$_2$), 1.19 (d, 3H, $CH(CH_3)_2$), 1.11 (d, 21 H, $CH(CH_3)_2$). ^{13}C NMR ($CDCl_3$, major isomer resonances only): δ 132.4 (C_{ipso}), 127.1 (C_{ortho}), 123.3 (C_{meta}), 118.5 (C_{para}), 28.0 (*C*HMe$_2$), 23.5 ($CH(CH_3)_2$).

---

(89) Guzei, I. A.; Liable-Sands, L. M.; Rheingold, A. L.; Winter, C. H. *Polyhedron* **1997**, *16*, 4017−4022.

(90) Gibson, V. C.; Reardon, D. F.; Tomov, A. K. WO 2004063233.

(91) Duff, A. W.; Hitchcock, P. B.; Lappert, M. F.; Taylor, R. G.; Segal, J. A. *J. Organomet. Chem.* **1985**, *293*, 271−283.

(L^1)$_2$Zn, 1. A suspension of L^{1}H (1.01 g, 2.76×10^{-3} mol) in 20 cm^3 toluene was added dropwise to a solution of ZnEt$_2$ (7.5 cm^3, 1.1 M in toluene, 8.29×10^{-3} mol, 3.0 equiv), which had previously been diluted with a further 20 cm^3 toluene, and was chilled to −78 °C. The reaction mixture was then allowed to warm to ambient temperature and stirred for a total of 18 h before volatile components were removed under reduced pressure. The crude product was recrystallized by allowing a saturated pentane solution to stand overnight (18 h) at −30 °C to give **1** as pale-yellow crystals (0.598 g, 7.53×10^{-4} mol, 55% yield based on L^{1}H). Crystals suitable for X-ray crystallography were grown by allowing a saturated pentane solution to stand at room temperature for several days. Anal. Calcd for $C_{48}H_{68}N_6Zn$: C 72.57, H 8.63, N 10.58. Found C 72.61, H 8.75, N 10.42. ^{1}H NMR (C_6D_6): δ 7.14−7.07 (m, 12H, H_{meta}, H_{para}), 3.48 (sept, 8H, $^3J_{HH}$ = 6.9 Hz, C*H*Me$_2$), 1.15 (d, 48H, $^3J_{HH}$ = 6.9 Hz, CH(C*H*$_3$)$_2$). ^{13}C NMR (C_6D_6): δ 143.80 (C_{ortho}), 141.49 (C_{ipso}), 127.04 (C_{para}), 123.59 (C_{meta}), 28.87 (*C*HMe$_2$), 23.76 (CH(*C*H$_3$)$_2$).

(L^1)$_2$Mg(Et$_2$O), 2. A 30 cm^3 Et$_2$O solution of L^{1}H (1.010 g, 2.76×10^{-3} mol) was added dropwise to a 10 cm^3 Et$_2$O solution of $^{n/s}$Bu$_2$Mg (2.90 mmol) chilled to −78 °C. The reaction mixture was stirred for 2 h at room temperature after which time the volatile components were removed under reduced pressure. The crude product was recrystallized by allowing a saturated heptane solution to stand at room temperature for 18 h to give **2** as pale-yellow crystals (0.657 g, 7.90×10^{-4} mol, 57% yield based on N[N(2,6-^{i}Pr$_2$C$_6$H$_3$)]$_2$H). Crystals suitable for X-ray crystallography were grown by allowing a saturated heptane solution to stand at room temperature for several days. Anal. Calcd for $C_{48}H_{68}N_6Mg$: C 76.52, H 9.10, N 11.15. Found C 76.37, H 9.20, N 11.16. ^{1}H NMR (C_6D_6): δ 7.18−7.12 (m, 12H, H_{meta}, H_{para}), 3.52 (br q, 4H, O(C*H*$_2$CH$_3$)$_2$), 3.30 (sept, 8H, $^3J_{HH}$ = 6.7 Hz, C*H*Me$_2$), 1.12 (d, 48H, $^3J_{HH}$ = 6.7 Hz, CH(C*H*$_3$)$_2$), 0.69 (t, 6H, $^3J_{HH}$ = 6.9 Hz, O(CH$_2$C*H*$_3$)$_2$). ^{13}C NMR (C_6D_6): δ 144.70 (C_{ipso}), 143.51 (C_{ortho}), 125.96 (C_{para}), 123.64 (C_{meta}), 64.93 (O(*C*H$_2$CH$_3$)$_2$), 28.60 (*C*HMe$_2$), 24.60 (CH(*C*H$_3$)$_2$), 13.57 (O(CH$_2$*C*H$_3$)$_2$).

(L^2)$_2$Zn, 3. A solution of L^{2}H (0.98 g, 2.60 mmol) in toluene (20 mL) was added dropwise to a solution of Zn[N(SiMe$_3$)$_2$]$_2$ (1.00 g, 2.60 mmol) in toluene (20 mL) cooled to −78 °C. The reaction was then stirred for 18 h while warming to room temperature, after which the volatile components were removed under reduced pressure. The crude product was recrystallized by cooling a saturated heptane solution from 60 °C to room temperature to afford **3** as colorless crystals (0.552 g, 0.67 mmol, 52% yield based on L^{2}H). Crystals suitable for X-ray crystallography were grown by slowly cooling a saturated heptane solution from 60 °C to room temperature. Anal. Calcd for $C_{52}H_{72}N_4Zn$: C 76.12, H 9.09, N 6.83. Found C 76.21, H 9.11, N 6.71. ^{1}H NMR (C_7D_8): δ 7.15−6.90 (m, 12H, C$_6$*H*$_3$), 3.53 (br, 4H, C*H*(CH$_3$)$_2$), 3.07 (br, 4H, C*H*(CH$_3$)$_2$), 1.33 (br, 12H, CH(C*H*$_3$)$_2$), 1.27 (s, 6H, C*H*$_3$), 1.13 (br, 24H, CH(C*H*$_3$)$_2$), 0.49 (br, 12H, CH(C*H*$_3$)$_2$). ^{13}C NMR (C_7D_8): δ 174.56 (N*C*N), 143.96 (2 + 6-*C*$_6$H$_3$), 141.87 (1-*C*$_6$H$_3$), 124.86 (3 + 5-*C*$_6$H$_3$), 123.31 (4-*C*$_6$H$_3$), 28.74 (*C*H(CH$_3$)$_2$), 23.87 (CH(*C*H$_3$)$_2$), 22.90 (br, CH(*C*H$_3$)$_2$), 14.16 (*C*H$_3$).

(L^2)$_2$Mg, 4. A solution of ^{n}BuLi (2.5 M in hexane, 1.10 mL, 2.76 mmol) was added to a solution of L^{2}H (1.042 g, 2.75 mmol) in toluene (30 mL) cooled to 0 °C. After being stirred for 3 h at room temperature, the mixture was cooled to −78 °C and a solution of ^{i}PrMgCl (2.0 M in Et$_2$O) (1.40 mL, 2.80 mmol) was added. The mixture was then stirred for 18 h while warming to room temperature. The colorless solution was filtered, and the solvent was removed under reduced pressure. The crude product was recrystallized by cooling a saturated heptane solution from 70 °C to room temperature to afford **4** as colorless crystals (0.761 g, 0.98 mmol, 71% yield based on L^{2}H). Crystals suitable for X-ray crystallography were grown by slowly cooling a saturated heptane solution from 70 °C to room temperature. Anal. Calcd for $C_{52}H_{74}N_4Mg$: C 80.13, H 9.57, N 7.19. Found C 80.02, H 9.68, N 7.10. ^{1}H NMR (C_6D_6): δ 7.06 (m, 12H, C$_6$*H*$_3$), 3.29 (br sept, 8H, C*H*(CH$_3$)$_2$), 1.37 (s, 6H, C*H*$_3$), 1.18 (d, 24H, $^3J_{HH}$ 6.8 Hz, CH(C*H*$_3$)$_2$), 1.03 (br, 24H, CH(C*H*$_3$)$_2$). ^{13}C NMR (C_6D_6): δ 176.81 (N*C*N), 143.14 (2 + 6-*C*$_6$H$_3$), 142.75 (1-*C*$_6$H$_3$), 124.72 (4-*C*$_6$H$_3$), 123.30 (3 + 5-*C*$_6$H$_3$), 28.84 (*C*H(CH$_3$)$_2$), 23.58 (CH(*C*H$_3$)$_2$), 14.97 (*C*H$_3$).

[(L^2)Zn$_2$Me$_2$]$_2$O, 5. A solution of L^{2}H (0.503 g, 1.32 mmol) in toluene (30 mL) was added dropwise to a solution of ZnMe$_2$ (2 M in toluene, 3.40 mL, 6.61 mmol) in toluene (30 mL) cooled to −78 °C. The mixture was then stirred for 3 h at room temperature, after which the volatile components were removed under reduced pressure. The crude product was recrystallized by cooling a hot heptane solution from 60 °C to room temperature to afford **5** as colorless crystals (0.203 g, 0.19 mmol, 29% yield based on L^{2}H). Crystals suitable for X-ray crystallography were grown by slowly cooling a hot heptane solution from 60 °C to room temperature. Despite repeated attempts, it was not possible to obtain satisfactory elemental analysis for this complex. ^{1}H NMR (C_6D_6): δ 7.10−7.03 (m, 12H, C$_6$*H*$_3$), 3.46 (sept, 8H, $^3J_{HH}$ 6.9 Hz, C*H*(CH$_3$)$_2$), 1.35 (s, 6H, C*H*$_3$), 1.31 (d, 24H, $^3J_{HH}$ 7.0 Hz, CH(C*H*$_3$)$_2$), 1.16 (d, 24H, $^3J_{HH}$ 6.9 Hz, CH(C*H*$_3$)$_2$), −0.47 (s, 12H, ZnC*H*$_3$). ^{13}C NMR (C_6D_6): δ 171.33 (NCN), 143.38 (1-*C*$_6$H$_3$), 143.26 (2 + 6-*C*$_6$H$_3$), 126.43 (4-*C*$_6$H$_3$), 124.17 (3 + 5-*C*$_6$H$_3$), 28.50 (*C*H(CH$_3$)$_2$), 24.17 (CH(*C*H$_3$)$_2$), 23.75 (CH(*C*H$_3$)$_2$), 19.17 (*C*H$_3$), −12.59 (Zn*C*H$_3$).

[(L^2)Zn$_2$Et$_2$]$_2$O, 6. A solution of L^{2}H (3.350 g, 8.85 mmol) in toluene (30 mL) was added dropwise to a solution of ZnEt$_2$ (1.1 M in toluene, 24.00 mL, 26.55 mmol) in toluene (30 mL) cooled to −78 °C. The mixture was then stirred for 3 h at room temperature, after which the volatile components were removed under reduced pressure. The crude product was recrystallized by cooling a saturated heptane solution from 60 °C to room temperature to afford **6** as colorless crystals (2.251 g, 1.96 mmol, 44% yield based on L^{2}H). Crystals suitable for X-ray crystallography were grown by slowly cooling a saturated heptane solution from 60 °C to room temperature. Anal. Calcd for $C_{60}H_{94}N_4Zn_4O$: C 62.72, H 8.25, N 4.88. Found C 62.61, H 8.12, N 4.84. ^{1}H NMR (C_6D_6): δ 7.12−7.05 (m, 12H, C$_6$*H*$_3$), 3.49 (sept, 8H, $^3J_{HH}$ 6.9 Hz, C*H*(CH$_3$)$_2$), 1.34 (d, 24H, $^3J_{HH}$ 6.9 Hz, CH(C*H*$_3$)$_2$), 1.33 (s, 6H, C*H*$_3$), 1.27 (t, 12H, $^3J_{HH}$ 8.1 Hz, ZnCH$_2$C*H*$_3$), 1.15 (d, 24H, $^3J_{HH}$ 6.9 Hz, CH(C*H*$_3$)$_2$), 0.41 (q, 8H, $^3J_{HH}$ 8.1 Hz, ZnC*H*$_2$CH$_3$). ^{13}C NMR (C_6D_6): δ 171.12 (NCN), 143.71 (1-*C*$_6$H$_3$), 143.40 (2 + 6-*C*$_6$H$_3$), 126.44 (4-*C*$_6$H$_3$), 124.27 (3 + 5-*C*$_6$H$_3$), 28.50 (*C*H(CH$_3$)$_2$), 24.40 (CH(*C*H$_3$)$_2$), 24.04 (CH(*C*H$_3$)$_2$), 19.08 (*C*H$_3$), 12.89 (ZnCH$_2$*C*H$_3$), 2.17 (Zn*C*H$_2$CH$_3$).

[(L^3)ZnCl(THF)], 7, and [(L^3)Zn(μ-Cl)]$_2$, 8. A solution of L^3-Li (3.030 g, 7.10 mmol) in THF (30 mL) was added dropwise to a solution of ZnCl$_2$ (0.985 g, 7.23 mmol) in THF (30 mL) cooled to −78 °C. The mixture was then stirred for 18 h while warming to room temperature. The colorless solution was filtered, and the solvent was then removed under reduced pressure. The crude product, (L^3)ZnCl(THF), **7**, was recrystallized by cooling a saturated toluene solution from 70 °C to −30 °C to afford {(L^3)Zn(μ-Cl)}$_2$, **8**, as colorless crystals (2.526 g, 4.85 mmol, 68% yield). Crystals suitable for X-ray crystallography were grown by allowing a saturated toluene solution to stand at room temperature for several days. Anal. Calcd for $C_{58}H_{86}N_4Zn_2Cl_2$: C 66.92, H 8.33, N 5.38. Found C 67.04, H 8.32, N 5.29. ^{1}H NMR (C_6D_6): δ 7.08−6.98 (m, 6H, C$_6$*H*$_3$), 4.06 (sept, 4H, $^3J_{HH}$ 6.8 Hz, C*H*(CH$_3$)$_2$), 1.27 (d, 12H, $^3J_{HH}$ 6.8 Hz, CH(C*H*$_3$)$_2$), 1.15 (d, 12H, $^3J_{HH}$ 6.8 Hz, CH-

(CH_3)$_2$), 0.93 (s, 9H, C(CH_3)$_3$). ^{13}C NMR (C_6D_6): δ 178.89 (N*C*N), 143.49 (2 + 6-*C*$_6$H$_3$), 142.18 (1-*C*$_6$H$_3$), 125.17 (4-*C*$_6$H$_3$), 123.39 (3 + 5-*C*$_6$H$_3$), 41.97 (*C*(CH$_3$)$_3$), 29.85 (C(*C*H$_3$)$_3$, 28.87 (*C*HCH$_3$)$_2$), 25.88 (CH(*C*H$_3$)$_2$), 22.34 (CH(*C*H$_3$)$_2$).

Synthesis of (L^3)ZnN(SiMe$_3$)$_2$, 9. A solution of KN(SiMe$_3$)$_2$ (0.216 g, 1.28 mmol) in toluene (20 mL) was added dropwise to a solution of **8** (0.530 g, 1.02 mmol) in toluene (20 mL) cooled to −78 °C. The mixture was then stirred for 18 h while warming to room temperature. The colorless solution was filtered, and the solvent was then removed under reduced pressure. The crude product was recrystallized by allowing a saturated heptane solution to stand at −30 °C for several days to afford (L^3)ZnN(SiMe$_3$)$_2$, **9**, as colorless crystals (0.273 g, 0.423 mmol, 42% yield). Anal. Calcd for $C_{35}H_{61}N_3Si_2Zn$: C 65.13, H 9.53, N 6.51. Found C 64.99, H 9.50, N 6.53. ^{1}H NMR (C_6D_6): δ 7.08−7.03 (m, 6H, C$_6$*H*$_3$), 6.58 (sept, 4H, $^3J_{HH}$ 6.9 Hz, C*H*(CH$_3$)$_2$), 1.32 (overlapping d, 12H, $^3J_{HH}$ 6.4 Hz, CH(C*H*$_3$)$_2$), 1.30 (overlapping d, 12H, $^3J_{HH}$ 6.4 Hz, CH(C*H*$_3$)$_2$), 0.95 (s, 9H, C(C*H*$_3$)$_3$), 0.11 (s, 18H, Si(C*H*$_3$)$_3$). ^{13}C NMR (C_6D_6): δ 180.75 (N*C*N), 142.93 (2 + 6-*C*$_6$H$_3$), 142.64 (1-*C*$_6$H$_3$), 125.43 (4-*C*$_6$H$_3$), 123.70 (3 + 5-*C*$_6$H$_3$), 41.75 (*C*(CH$_3$)$_3$), 29.97 (C(*C*H$_3$)$_3$, 28.89 (*C*HCH$_3$)$_2$), 25.26 (CH(*C*H$_3$)$_2$), 22.66 (CH(*C*H$_3$)$_2$), 5.58 (Si(*C*H$_3$)$_3$).

Synthesis of (L^3)Mg^{i}Pr(Et$_2$O), 10. A solution of ^{i}PrMgCl (2 M in Et$_2$O, 1.45 mL, 2.90 mmol) was added dropwise to a solution of L^{3}Li (1.211 g, 2.84 mmol) in diethyl ether (30 mL) cooled to −78 °C. The mixture was then stirred for 18 h while warming to room temperature, after which the solvent was removed under reduced pressure and the product was extracted into toluene (30 mL). After the removal of the solvent, the crude product was recrystallized by allowing a saturated heptane solution to stand at room temperature for 18 h to afford (L^3)Mg^{i}Pr(Et$_2$O), **10**, as colorless crystals (0.820 g, 1.46 mmol, 51% yield). Crystals suitable for X-ray crystallography were grown by allowing a saturated heptane solution to stand at room temperature for several days. Despite repeated attempts it was not possible to obtain satisfactory elemental analysis for this complex. ^{1}H NMR (C_6D_6): δ 7.15−7.04 (m, 6H, C$_6$*H*$_3$), 3.69 (sept, 4H, $^3J_{HH}$ 6.8 Hz, C*H*(CH$_3$)$_2$), 2.97 (q, 4H, $^3J_{HH}$ 7.1 Hz, O(C*H*$_2$CH$_3$)$_2$), 1.78 (d, 6H, $^3J_{HH}$ 7.8 Hz, MgCH(C*H*$_3$)$_2$), 1.42 (d, 12H, $^3J_{HH}$ 6.9 Hz, CH(C*H*$_3$)$_2$), 1.26 (d, 12H, $^3J_{HH}$ 6.7 Hz, CH(C*H*$_3$)$_2$), 1.03 (s, 9H, C(C*H*$_3$)$_3$), 0.71 (t, 6H, $^3J_{HH}$ 7.1 Hz, O(CH$_2$C*H*$_3$)$_2$), 0.34 (sept, 1H, $^3J_{HH}$ 7.8 Hz, MgC*H*(CH$_3$)$_2$). ^{13}C NMR (C_6D_6): δ 178.97 (N*C*N), 145.28 (1-*C*$_6$H$_3$), 141.94 (2 + 6-*C*$_6$H$_3$), 123.46 (3 + 5-*C*$_6$H$_3$), 123.40 (4-*C*$_6$H$_3$), 66.89 (O(*C*H$_2$-CH$_3$)$_2$), 44.71 (*C*(CH$_3$)$_3$), 31.12 (C(*C*H$_3$)$_3$), 28.57 (*C*H(CH$_3$)$_2$), 25.77 (CH(*C*H$_3$)$_2$), 25.08 (MgCH(*C*H$_3$)$_2$), 23.07 (CH(*C*H$_3$)$_2$), 13.62 (O(CH$_2$*C*H$_3$)$_2$), 10.71 (Mg*C*H(CH$_3$)$_2$).

Synthesis of (L^3)Mg^{i}Pr(THF), 11. 11 was prepared in a similar manner to that outlined for **10**, but using L^{3}Li (1.035 g, 2.41 mmol), ^{i}PrMgCl (2.0 M in THF, 1.21 mL, 2.41 mmol), and THF as a solvent. The crude product was recrystallized by allowing a saturated heptane solution to stand at −30 °C for 18 h to afford (L^3)Mg^{i}Pr(THF), **11**, as colorless crystals (0.493 g, 0.882 mmol, 37% yield). Anal. Calcd for $C_{32}H_{80}N_2Mg(C_4H_8O)$: C 77.33, H 10.46, N 5.01. Found C 77.53, H 10.72, N 5.37. ^{1}H NMR (C_6D_6): δ 7.15−7.05 (m, 6H, C$_6$*H*$_3$), 3.68 (sept, 4H, $^3J_{HH}$ 6.9 Hz, C*H*(CH$_3$)$_2$), 3.49 (br m, 4H, THF), 1.68 (d, 6H, $^3J_{HH}$ 7.9 Hz, MgCH(C*H*$_3$)$_2$), 1.40 (d, 12H, $^3J_{HH}$ 6.9 Hz, CH(C*H*$_3$)$_2$), 1.25 (d, 12H, $^3J_{HH}$ 6.7 Hz, CH(C*H*$_3$)$_2$), 1.12 (br m, 4H, THF), 1.01 (s, 9H, C(C*H*$_3$)$_3$), 0.45 (sept, 1H, $^3J_{HH}$ 7.8 Hz, MgC*H*(CH$_3$)$_2$). ^{13}C NMR (C_6D_6): δ 179.21 (N*C*N), 145.31 (1-*C*$_6$H$_3$), 142.14 (2 + 6-*C*$_6$H$_3$), 123.41 (4-*C*$_6$H$_3$), 123.22 (3 + 5-*C*$_6$H$_3$), 69.53 (THF), 44.41 (*C*(CH$_3$)$_3$), 30.89 (C(*C*H$_3$)$_3$), 28.69 (*C*H(CH$_3$)$_2$), 26.03 (CH(*C*H$_3$)$_2$), 25.25 (THF), 24.99 (MgCH(*C*H$_3$)$_2$), 22.63 (CH(*C*H$_3$)$_2$), 9.55 (Mg*C*H(CH$_3$)$_2$).

Acknowledgment. This work was supported by scholarships from the Institute for the Promotion of Teaching Science and Technology (IPST), Thailand (to N.N. and P.T.).

Supporting Information Available: Full details of the crystallographic analysis of **1**−**6**, **8**, and **10** (including additional figures) and CIF files. This material is available free of charge via the Internet at http://pubs.acs.org.

IC701061Q